

Automatic Seismic Salt Interpretation with Deep Convolutional Neural Networks

Yu Zeng^{1†}, Kebei Jiang², and Jie Chen³

¹ yu.zeng@alumni.duke.edu

² kebei.jiang13@gmail.com

³ jie.ch.2000@gmail.com

† Corresponding author

December 5, 2018

Abstract

One of the most crucial tasks in seismic reflection imaging is to identify the salt bodies with high precision. Traditionally, this is accomplished by visually picking the salt/sediment boundaries, which requires a great amount of manual work and may introduce systematic bias. With recent progress of deep learning algorithm and growing computational power, a great deal of efforts have been made to replace human effort with machine power in salt body interpretation. Currently, the method of Convolutional neural networks (CNN) is revolutionizing the computer vision field and has been a hot topic in the image analysis. In this paper, the benefits of CNN-based classification are demonstrated by using a state-of-art network structure U-Net, along with the residual learning framework ResNet, to delineate salt body with high precision. Network adjustments, including the Exponential Linear Units (ELU) activation function, the Lovász-Softmax loss function, and stratified K -fold cross-validation, have been deployed to further improve the prediction accuracy. The preliminary result using SEG Advanced Modeling (SEAM) data shows good agreement between the predicted salt body and manually interpreted salt body, especially in areas with weak reflections. This indicates the great potential of applying CNN for salt-related interpretations.

1 Introduction

Salt, whenever it is present, plays an important role (Jones and Davison, 2014) in seismic reflection imaging due to its distinctive acoustic features and usually complex shape. One of the major tasks in seismic imaging and interpretation is then to precisely distinguish salt-bodies from surrounding sediment. In most cases, salt-body possesses a clear boundary and is easy to be identified with human vision. However, seismic data tends to be massive (TB level) and it is not uncommon to have a group of people working for weeks to finish a full-survey salt-body delineating. The clear definition of salt-body and overwhelming amount of data actually makes this challenge a perfect task for deep learning.

Deep learning, which is capable of extracting extremely detailed features from given data, has had a huge impact on the development of image analysis, especially, semantic segmentation. Recently, deep learning found its application in oil and gas industry, such as well log correlation, fault interpretation (Maniar et al., 2015) and rock facies classification (Chen and Zeng, 2018). Convolutional Neural Network (CNN), being one of the most powerful 'weapons' in the deep learning arsenal, utilizes numerous convolving/pooling/activation layers to obtain a collection of underlying features from the original image. The effectiveness of CNN in salt-body identification has been shown in a recent study (Di et al., 2018), where a proof-of-principle study focusing on factors contributing to the superiority of CNN has been provided.

In this paper, we aim to extend on the work by utilizing the state-of-art CNN with U-Net architecture to fully exploit its potential in regards to salt-body identification. We will first describe the deployed convolutional network structure, and then discuss the adjustments we have made to improve the network training. Finally, we will show the preliminary salt interpretation result and will have some discussions on its possible applications and how to further improve.

2 Training and Testing Data

The dataset we used for this study is the SEG Advanced Modeling (SEAM) Phase 1 data (SEAM, 2009) that emphasizes on deep-water Gulf of Mexico and contains complex salt geometries. The salt body on inline number 4403, 4499, and 4595 is manually interpreted by Dr. Haibin Di as in Ref. (Di et al., 2018). Both seismic images and corresponding salt body masks are then splitted into small pieces with each piece 101×101 pixel in size. For this study, small image pieces from inline 4403 and 4499 are used as training/development set. The small image pieces from inline 4595 are used as testing set. Augmentation including flipping of axes, tilting, rotation and scaling is applied to simulate a larger training sample and to prevent the network from possible overfitting. The seismic images and corresponding salt body labels for these three inlines are shown in Fig. 1.

3 Network Architecture

The U-Net (Ronneberger et al., 2015) structure, which combines a contracting/down-sampling path to extract context information (what) and a symmetric expanding/up-sampling path to retrieve location information (where), has been used as our baseline architecture. To overcome the degradation problem with deep learning networks, a particular advanced variant of U-Net is adopted in our experiments: the Deep Residual Learning or the ResNet (He et al., 2015). ResNet is constructed by adding an identity mapping shortcut on top of every few stacked layers. This will result in higher prediction precision due to the fact that it is easier to learn the mapping of the perturbation, which is close to zero, than directly learn from the full input. A schematic view of U-Net architecture is shown in Fig. 2.

4 Evaluation Metric

In our experimentation, the intersection-over-union (IoU) score, also known as Jaccard index, is used to quantify the performance of CNN salt identification, which is the more widely accepted evaluation

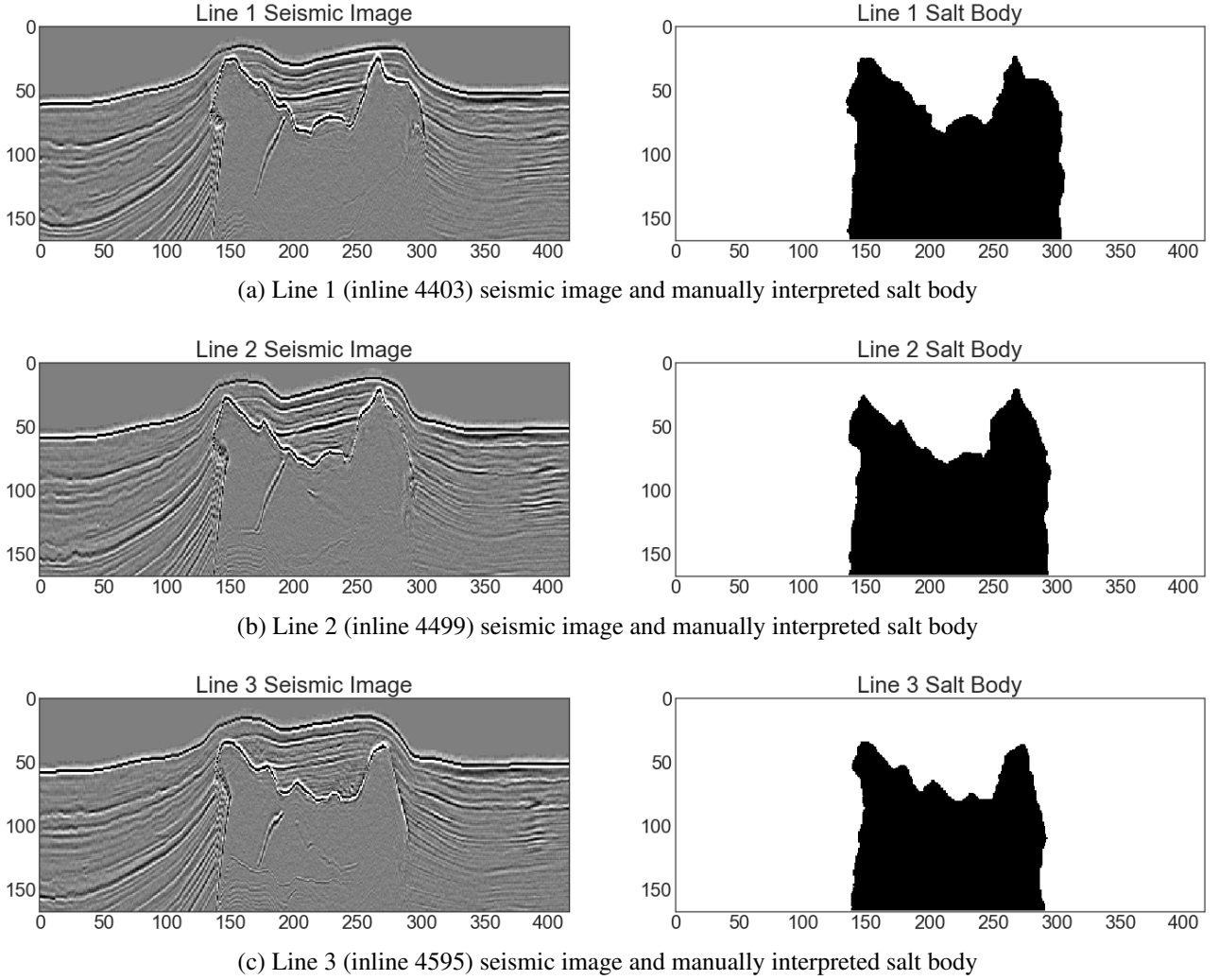


Figure 1: Seismic image (left) and the corresponding manually interpreted salt body (right). For salt body interpretation, black color is for salt and white color is for non-salt. Line 1 and 2 are used in training/development; Line 3 is used in testing.

matrix in the image segmentation. IoU measures similarity between two or more definitive sample sets. Mathematically, it can be written as the intersection divided by the union of the sample sets.

$$J(A, B) = \frac{A \cap B}{A \cup B} \quad (1)$$

This generates a statistic measure between 0 to 1, with convention of 1 for case 0/0, in a binary segmentation problem. High IoU score (closer to 1) indicates the higher similarity of the two sample sets, thus higher performance of CNN in salt identification. Specifically in this case, higher IoU score means better consistence between the predicted salt pixels and the ground truth salt mask.

5 Network Training

In addition to utilizing the state-of-art U-Net + ResNet network structure with conventional configuration for deep neural networks, which includes He initialization (He et al., 2015) that particularly

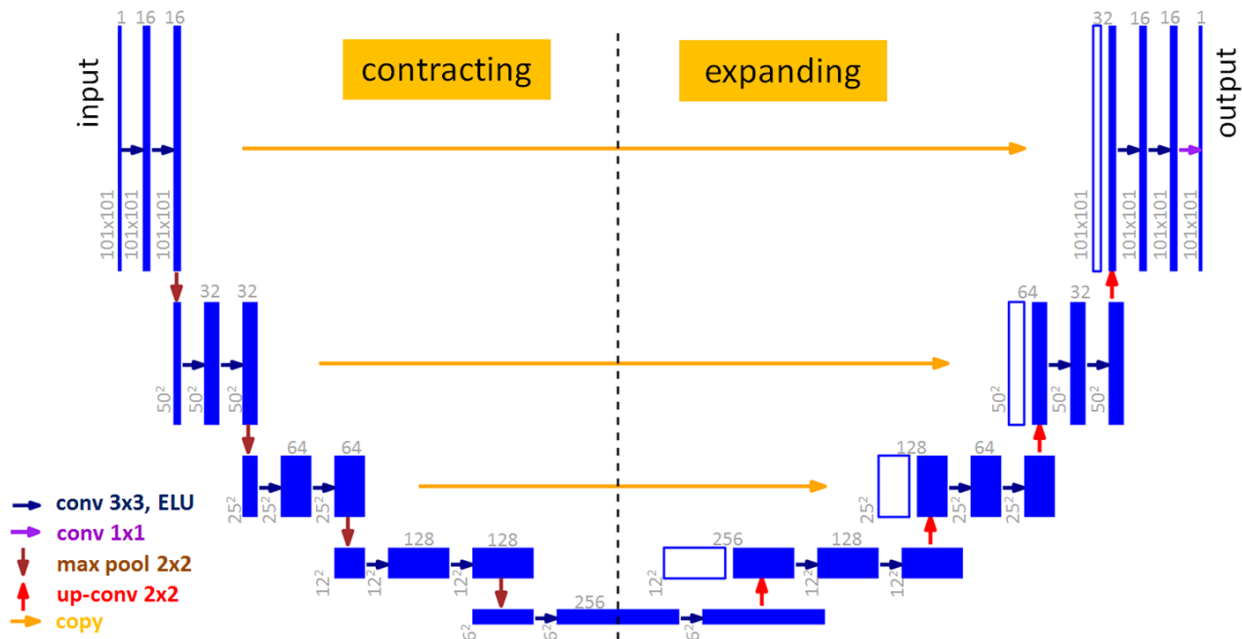


Figure 2: A schematic view of U-Net architecture. Blue box on left corresponds to a multi-channel feature map in contracting path, where the number of channels increases stage by stage. On contrary, blue box on right corresponds to a multi-channel feature map in an expansive path, where the number of channels decreases stage by stage. The horizontal arrow denotes the transfer of residual information from layers in the contracting path to the corresponding layers in the expansive path.

considers the rectifier nonlinearities, batch normalization and dropout, a few adjustments of the network were implemented to further improve the salt body prediction precision.

Firstly, a stratified K-folding cross-validation is implemented to split the training data into groups with roughly the same proportions of salt/non-salt images. Compared to regular cross-validation, Stratified cross-validation usually leads to results with smaller bias/variance and therefore better generalization. Secondly, while the standard ReLU activation function may cause some units not being activated at all, we choose to use ELU (Clevert et al., 2015) as it acknowledges small negative values while heavily penalizes large ones. Lastly, we will justify the addition of training epochs in respect to Lovász-Softmax loss. The Jaccard index, or commonly known as the intersection-over-union (IoU) score is broadly accepted as the best evaluation of the precision of image segmentation as demonstrated in (Berman et al., 2018). We also promoted the Lovász-Softmax loss function as an effective surrogate for IoU optimization. Given the fact that the IoU measure is sensitive to hyperparameters such as learning rates and batch sizes, we will train our network initially using cross-entropy loss to locate optimal hyperparameters prior to training against the Lovász-Softmax loss for fine-tuning.

5.1 Stratified K-Fold

The K -fold cross-validation means splitting the training dataset into K -folds, then train on $K - 1$ folds and make predictions and evaluations on the remaining 1 fold. The stratified K -fold sampling is performed to produce folds that contain a representative ratio of each class and is thus a better way to split training data. As discussed in many machine learning literatures, model averaging is a quite powerful and reliable way to reduce generalization errors. The reason why model averaging can

further improve the evaluation score is that different models will unlikely make all the same errors on the test set. Assume each of the K models makes an error δ_i on each event and δ_i is randomly drawn from a Gaussian distribution with $\mathbb{E}[\delta_i] = 0$, $\mathbb{E}[\delta_i^2] = Var$ and $\mathbb{E}[\delta_i\delta_j] = Cov$. The expected variance of ensemble model will be described by Eqn.2:

$$\mathbb{E} \left[\frac{1}{K} \left(\sum_i \delta_i \right)^2 \right] = \frac{1}{K^2} \mathbb{E} \left[\sum_i \left(\delta_i^2 + \sum_{j \neq i} \delta_i \delta_j \right) \right] = \frac{Var}{K} + \frac{(K-1) \cdot Cov}{K} \quad (2)$$

In the case where errors are independent, covariance Cov will be 0 and Eqn.2 can be simplified as:

$$\mathbb{E} \left[\frac{1}{K} \left(\sum_i \delta_i \right)^2 \right] = \frac{Var}{K} \quad (3)$$

If errors are perfectly correlated, variance and covariance will be identical and Eqn.2 can be simplified as:

$$\mathbb{E} \left[\frac{1}{K} \left(\sum_i \delta_i \right)^2 \right] = Var \quad (4)$$

If errors are partially correlated, the expected variance of ensemble model will be within the two extreme values:

$$\frac{Var}{K} < \mathbb{E} \left[\frac{1}{K} \left(\sum_i \delta_i \right)^2 \right] < Var \quad (5)$$

For neural networks, the differences in random initialization, random mini-batch selection, and differences in hyperparameter space will tend to make prediction errors from different folds to be partially independent. As demonstrated in Eqn.5, the ensemble of the K models will, on average, perform better than its member models if the errors are not perfectly correlated.

We have tested stratified K -fold training and prediction with $K = 5$. The final prediction is the average of the prediction results from 5 models. By comparing with the result not using stratified K -fold, we observe a ~ 0.015 improvement in the evaluation score given sufficiently large (~ 500) training epochs.

5.2 Activation Function

In neural networks, the activation function of a node is a mathematical function which calculates the output of that node given an input or a set of inputs. The node output will be further used as input for subsequent layers until a desired solution is obtained.

For deep neural networks, one of the known issues is the tricky problem of *Vanishing Gradients*. Backpropagation algorithm will compute the gradient of the cost function with regards to each network parameter. In a *Gradient Descent* step, these gradients will then be used to update each parameter. However, as the algorithm progresses to the lower layers, the gradients often get smaller and then the parameters are virtually not updated. A poor choice of activation function will make the issue of *Vanishing Gradients* even worse. Recent studies (Glorot and Bengio, 2010; Kawaguchi, 2016) have demonstrated the *Rectified Linear Unit* (ReLU) activation function is better than sigmoid activation function. The ReLU activation function is not only fast to compute but also does not saturate for positive values. Its definition is given by Eqn.6 and is represented in Figure 3 (a).

However, the ReLU activation function still has limitations. One issue of ReLU is that during training, some nodes will only output 0 and will be effectively dead. To overcome this issue of *dying ReLUs*, variants of ReLU and other non-ReLU-type activation functions have been proposed. Among those, the *Exponential Linear Unit* (ELU) (Clevert et al., 2015) activation function is demonstrated to outperform all the ReLU variants. Figure 3 (b) and Eqn.7 gives ELU function's distribution and definition, respectively.

Comparing with the ReLU function, the ELU function has the following characteristics:

- For $x < 0$, the ELU function has non-zero gradient and thus fix the issue of dying nodes observed in the ReLU function.
- The ELU function is smooth everywhere even at $x = 0$. This may help to speed up the *Gradient Descent* calculation.
- The ELU function generally converges faster than the ReLU-type functions during training.
- Due to its exponential nature, the ELU function is generally slower in computation than the ReLU function and its variants.

In this seismic salt interpretation experiment, the ReLU function is initially used for the first 500 training epochs for better runtime performance. For later trainings, the ELU activation function is used instead. Comparing with using the ReLU function only, we found the switch from ReLU to ELU can improve the IoU score by ~ 0.002 .

$$\text{ReLU}(x) = \begin{cases} 0 & \text{if } x < 0 \\ x & \text{if } x \geq 0 \end{cases} \quad (6)$$

$$\text{ELU}_\alpha(x) = \begin{cases} \alpha \cdot (e^x - 1) & \text{if } x < 0 \\ x & \text{if } x \geq 0 \end{cases} \quad (7)$$

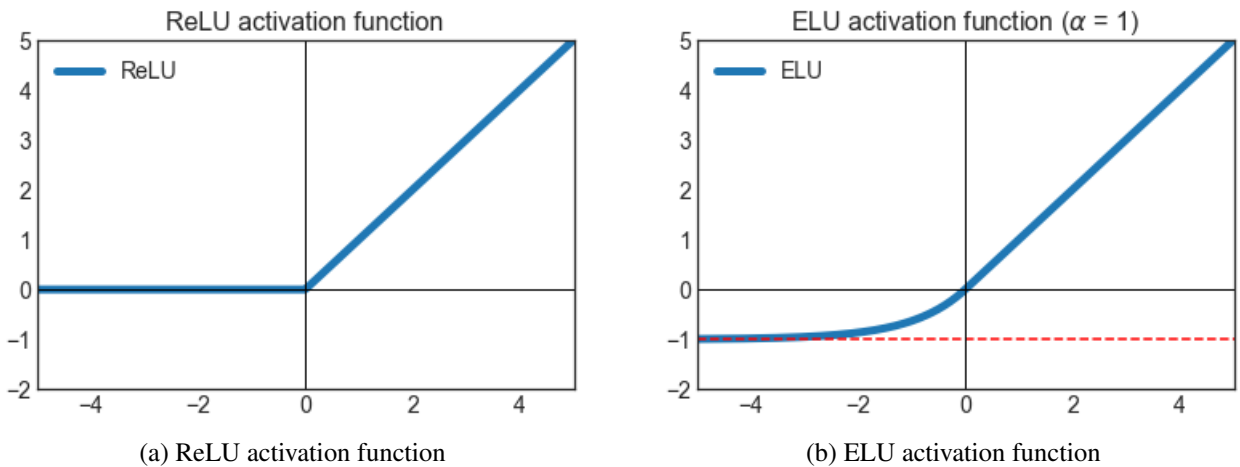


Figure 3: Comparison of the ReLU and the ELU activation functions

5.3 Loss Function

Conventional choice of loss function for neural network is to optimize the cross-entropy (Goodfellow et al., 2016) based on logistic regression. Complementary to the IoU score (or Jaccard index), Jaccard loss, obtained by subtracting the IoU score from 1, can be used to measure dissimilarity between sample sets and has been shown to be a better evaluation for image segmentation tasks (Berman et al., 2018). Therefore, maximizing IoU score is equivalent to minimizing Jaccard loss. The latter can be constructed as the loss function for the image segmentation.

It is well known that convex surrogate loss functions are essential to the practical application of empirical loss minimization (Yu and Blaschko, 2015). The issue of Jaccard loss is submodular. In other words, the Jaccard loss doesn't converge very well. To this end, Ref. (Berman et al., 2018) applies the Lovász hinge (Yu and Blaschko, 2015) as a good surrogate to Jaccard loss, and yields a consistent improvement in capturing the absolute minimum of the Jaccard loss. The test datasets with this Lovász hinge Jaccard loss in the same reference shows benefits like better recovery of small objects and filling more gaps inside a large continuum. Lovász hinge Jaccard loss function can be generalized to multi-class classification problem as Lovász-Softmax loss function by considering the class-averaged IoU metric (mIoU):

$$loss(f) = \frac{1}{|C|} \sum_{c \in C} \overline{\Delta_{J_c}}(m(c)) \quad (8)$$

where Δ_{J_c} is the loss surrogate, $m(c)$ corresponds to the vector of pixel identification errors, and c is one subclass of multiple classes of C . Comparing with the usage of conventional cross-entropy loss, we find the usage of the Lovász-Softmax loss can improve the prediction accuracy by ~ 0.002 .

Though Lovász-Softmax loss function used in the U-Net has been shown (Rakhlin et al., 2018) to alleviate obstacles in computing vision classification task, like small amount of data, incomplete or mislabeling, and highly imbalanced classes, it is however, as discussed in Ref. (Berman et al., 2018), sensitive to hyper-parameters such as learning rates and batch sizes. In our trainings, cross-entropy loss is thus first used to make hyper-parameters converge toward optimal values. Later, in fine-tuning stage, the Lovász-Softmax loss is used in order to achieve better prediction accuracy.

5.4 Learning Rate Scheduling

The ideal learning rate has the advantage of learning quickly and converge to optimal solution. However, finding a good learning rate can be tricky. In this salt body interpretation experiment, we adopted a simple strategy called *predetermined piecewise constant learning rate*. The initial learning rate is set to $\eta_1 = 0.001$ for the first 500 epochs, then to $\eta_2 = 0.0005$ for the next 400 epochs and to $\eta_3 = 0.0001$ for the next 100 epochs. For each learning rate scenario, the best trained models are saved and are later reloaded for a different learning rate scenario. Table 1 summarizes key training parameters and algorithms for different training epochs. Training and validation score curves as a function of training epoch number are shown in Figures 4, 5 and 6. A general trend of improved IoU score with more training epochs is observed.

6 Results

To assess the quality of the automatic seismic interpretation, the best trained stratified 5-fold models are averaged and applied to the testing inline 4595. The comparison of its salt body prediction and a

Training Epoch	Learning Rate	Loss Function	Algorithm
1-500	0.001	Cross Entropy	Adam
501-900	0.0005	Lovász	Adam
901-1000	0.0001	Lovász	Adam

Table 1: Learning rate, loss function and algorithm used for different training epochs.

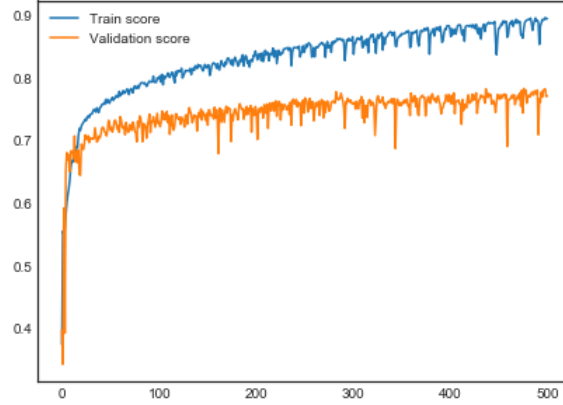


Figure 4: Train score and validation score for 500 training epochs using cross-entropy loss and learning rate $\eta_1 = 0.001$

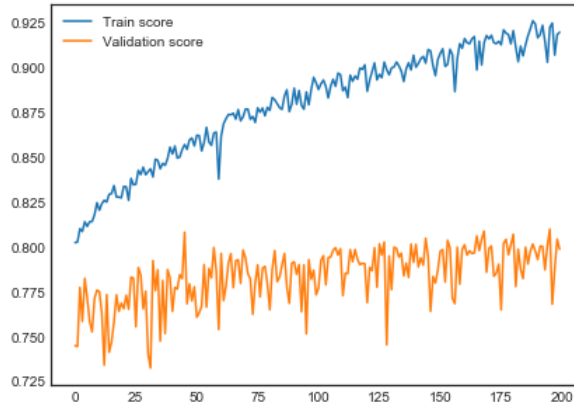


Figure 5: Train score and validation score for the first 200 training epochs using Lovász loss and learning rate $\eta_2 = 0.0005$

manual interpretation is shown in Fig. 7.

Overall, the general salt body shape predicted by CNNs agrees quite well with manual interpretation. This demonstrates the great potential in computer-aided seismic interpretation using the CNNs. We also notice that details at salt boundaries, though quite similar as manual interpretation, are not identical in some local places. What's more, areas with weak seismic reflection, for example block 879 in Fig. 7, may still suffer from mis-classification.

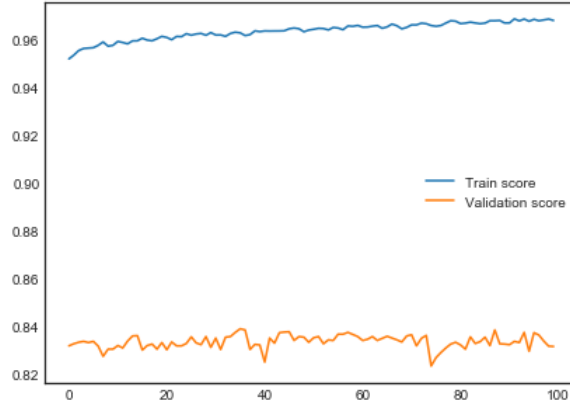


Figure 6: Train score and validation score for 100 training epochs using Lovász loss and learning rate $\eta_3 = 0.0001$

7 Discussion

For the relatively complex CNN architecture we have adopted and given the inputs we already have, we find the major improvements are mostly coming from more training epochs. In comparison, though the IoU improvements introduced by using ELU activation function and by using Lovász loss function are relatively small (~ 0.002 improvement for each), it is however robust and non-negligible. Ensemble method using stratified K -fold can further improve the test score by ~ 0.015 .

We would expect more training samples, the usage of pre-trained networks (i.e. ResNet34), and the implementation of snapshot ensemble would further improve the prediction accuracy. To speed up the training process and make the models converge faster, strategy of cyclic learning rate could be adopted to further improve. Another possible way to further improve, is by constructing edge detection related features as additional channel for the CNN.

At current stage, the CNN-based salt body interpretation is still not perfect and cannot replace manual interpretation. However, the implementation of deep CNNs on seismic data for salt body identification is still promising. For example, the rough salt body derived from CNN can be used as input for *Full Waveform Inversion* (Wang et al., 2018) without the need to manually interpret a salt body. Another possible application of this CNN-based method would be the real-time feature segmentation.

8 Conclusion

We have implemented a deep CNN-based architecture for automatic seismic data salt body interpretation. The network structure is based on U-net plus ResNet using the Adam algorithm. A few improvements, including ELU activation function, Lovász cost function, stratified K -fold cross validation and model averaging, have been made to further improve the salt body prediction accuracy. We have demonstrated that salt body can be successfully delineated using seismic data alone in an automatic manner and the prediction result is confirmed to agree well with a manually interpreted salt body.



Figure 7: Comparison of manual interpretation and CNN-based prediction with 1000 training epochs.

9 ACKNOWLEDGMENTS

The authors would like to thank SEG Advanced Modeling Corporation for providing SEAM data available for public usage, and Dr. Haibin Di for providing the training and the testing datasets used for this R&D. The neural network algorithm is implemented using the open-source Tensorflow package developed by Google.

References

- Jones, I. and I. Davison, 2014, Seismic Imaging In and Around Salt Bodies. Interpretation, Vol. 2, No. 4.
- Maniar, H., S. Ryali, M. S. Kulkarni, and A. Abubakar, 2018, Machine Learning Methods in Geoscience. SEG International Exposition and 88th Annual Meeting, page 4638-4642.

- Chen, J. and Y. Zeng, 2018, Application of Machine Learning in Rock Facies Classification with Physics-Motivated Feature Augmentation, arXiv:1808.09856
- Di, H., Z. Wang, and G. AlRegib, 2018, Why using CNN for Seismic Interpretation? An Investigation. SEG International Exposition and 88th Annual Meeting, page 2216-2220.
- Abriel, W., 2009, Overview of SEAM Initiative, SEAM workshop presentations: Presented at the 79th Annual International Meeting, SEG.
- Ronneberger, O., P. Fischer, and T. Brox, 2015, U-Net: Convolutional Networks for Biomedical Image Segmentation, arXiv:1505.04597
- He, K., X. Zhang, S. Ren, and J. Sun, 2015, Deep Residual Learning for Image Recognition, arXiv:1512.03385
- He, K., X. Zhang, S. Ren, and J. Sun, 2015, Delving Deep into Rectifiers: Surpassing Human-Level Performance on ImageNet Classification, arXiv:1502.01852
- Clevert, D., T. Unterthiner, and S. Hochreiter, 2015, Fast and Accurate Deep Network Learning by Exponential Linear Units (ELUs), arXiv:1511.07289
- Glorot, X. and Y. Bengio, 2010, Understanding the Difficulty of Training Deep Feedforward Neural Networks. In AISTATS, 2010.
- Kawaguchi, K., 2016, Deep Learning without Poor Local Minima, in Advances in Neural Information Processing Systems 29, 2016, page 586-594.
- Berman, Maxim and Rannen Triki, Amal and Blaschko, Matthew B., 2018, The Lovász-Softmax Loss: A Tractable Surrogate for the Optimization of the Intersection-Over-Union Measure in Neural Networks. The IEEE Conference on Computer Vision and Pattern Recognition (CVPR).
- Goodfellow, I., Bengio, Y., and Courville, A., 2016, Deep Learning. MIT Press
- Waldeland, A. U., A. C. Jensen, L-J. Gelius, and A. H. S. Solberg, 2018, Convolutional Neural Networks for Automated Seismic Interpretation. The Leading Edge, page 529-537.
- Yu, J. and M. B. Blaschko. Learning submodular losses with the Lovász hinge. In Proceedings of the 32nd International Conference on Machine Learning, volume 37 of Journal of Machine Learning Research: W&CP, pages 1623-1631, Lille, France, 2015.
- Rakhlin, A., A. Davydov, and S. Nikolenko, 2016, Land Cover Classification From Satellite Imagery With U-Net and Lovász-Softmax Loss. The IEEE Conference on Computer Vision and Pattern Recognition (CVPR) Workshops.
- Wang, P., Z. Zhang, Z. Wei and R. Huang, 2018, A Demigration-based Reflection Full Waveform Inversion Workflow. SEG Technical program Expanded Abstracts 2018, page 1138-1142.